



Research Article

Zinc Oxide Nanoparticles Induce Apoptosis in Human Breast Cancer Cells via Caspase-8 and P53 Pathway

Haitham Ali Kadhem¹, Sumayah Abdulhussien Ibraheem¹, Majid Sakhi Jabir²✉, Afraa Ali Kadhim³, Zainab Jihad Taqi², Mihailescu Dan Florin¹

¹Department of Animal Physiology and Biophysics, Faculty of Biology, Bucharest, Romania.

²Department of Applied Science, University of Technology, Baghdad, Iraq.

³Department of Biology, College of Science, University of Al-Mustansiriyah, Baghdad, Iraq.

✉ Corresponding author. E-mail: msj_iraq@yahoo.com

Received: May 18, 2018; **Accepted:** Nov. 19, 2018; **Published:** Feb. 28, 2019.

Citation: Haitham Ali Kadhem, Sumayah Abdulhussien Ibraheem, Majid Sakhi Jabir, Afraa Ali Kadhim, Zainab Jihad Taqi, and Mihailescu Dan Florin, Zinc Oxide Nanoparticles Induce Apoptosis in Human Breast Cancer Cells via Caspase-8 and P53 Pathway. *Nano Biomed. Eng.*, 2019, 11(1): 35-43.

DOI: 10.5101/nbe.v11i1.p35-43.

Abstract

Nanoparticles are a special institution of substances with precise capabilities and significant applications in many biomedical fields. In the present work zinc oxide nanoparticles were prepared through sol-gel approach. The synthesised nanoparticles were identified through the usage of X-ray powder diffraction (XRD), scanning electron microscopy (SEM) and transmission electron microscopy (TEM). In-vitro anticancer activity of zinc oxide nanoparticles towards MCF-7 cell lines using numerous parameters was investigated. Zinc oxide nanoparticles were determined to exert cell growth arrest against MCF-7 cell lines. The anti-proliferative efficiency of ZnO nanoparticles was due to cell dying and inducing apoptosis that were confirmed by the usage of acridine orange/ethidium bromide dual staining, DAPI staining and genotoxicity assay. Reverse transcription polymerase chain reaction (RT-PCR) analysis achieved to identify the gene expression of Caspase-8, Caspase-9, and P53. The results suggested that ZnO nanoparticles might find a wide use in clinical applications and provide new drug recompense for chemotherapy drugs.

Keywords: Zinc oxide nanoparticles; Cytotoxicity; MCF-7; Genotoxicity; Caspase-8; P53

Introduction

Among women, breast cancer is the leading cause of cancer deaths and the most common cancer worldwide. Globally, 1.3 million new cases of breast cancer are diagnosed and approximately 465,000 deaths are recorded annually [1]. Cancer may be outlined as a disease within which a variety of abnormal

cells develop uncontrollably irrespective to the traditional rules of cell division [2]. Traditional cells are perpetually controlled by signals that determine whether or not the cell ought to divide, differentiate into another cell or die. Among women, breast cancer is the leading cause of cancer deaths and the most common cancer worldwide. The exact cause of cancer is unidentified. Although the genetic aspect is

involved in five to ten percent of cancers, other reasons including poor diet, certain infection, lack of physical activity, obesity, the use of tobacco and pollution may also directly or indirectly influence the activity of crucial genes that could lead to cancer development [3]. In the last few years, scientists have used a new pathway for treating cancer, dependent on the concept of nanotechnology [4]. Nanotechnology is a science based on the techniques and tools from diverse disciplines, including biology, chemistry, engineering and medicine. This field could critically improve the drug bioavailability, and in turn reduce the toxicity associated with the high doses that are typically required for optimum response and ability to transport the substance on a specific organ [5]. Materials in nanoscale have attracted the attention of many researchers, and as a result entered in wide applications in fabricating stronger materials, high memory capacity, smaller electronics, advanced medical treatments and enhanced sensors [6]. Nanoparticles (NPs) possess the properties as connections between atomic structures and bulk materials, which makes them very interesting. Zinc oxide (ZnO) is one of the most usual metallics used commercially that are produced via artificial techniques [7]. ZnO is safe and well suited with human pores and skin by developing an appropriate additive for textiles and surfaces which might be in touch with flesh. In assessment to bulk, the growing quantity of nanoscale ZnO has the potential to decorate the efficiency of material operation [8]. As a critical semiconductor with remarkable medical and technological interest, ZnO-NPs are extensively applied in numerous commercial areas together with ultra-violet (UV) light-emitting devices, ethanol gas

sensors, image-catalysts, pharmaceutical and cosmetic industries [9, 10]. The purpose of this study is to manufacture Zinc oxide nanoparticles depending on sol-gel method and their characters were studied, and their activity against breast cancer cell line were investigated.

Experimental

Preparation of zinc oxide nanoparticles

The synthesis of zinc oxide nanoparticles was accomplished depending on Khan, et al. [11] with some modification (Fig. 1). Zinc acetate dehydrate ($4.16 \text{ g per } 100 \text{ mL}^{-1}$) was prepared with distal water. Sodium hydroxide ($3.5 \text{ g per } 100 \text{ mL}^{-1}$) was prepared using deionised water. Solution of sodium hydroxide was dropping above the prepared zinc acetate solution until obtaining pH scale range to 12. The mixture compound required further stirring for 1 h until the precipitate was seen. The precipitation was washed using deionised water and then filtered and dried overnight in the hot air oven at $70 \text{ }^\circ\text{C}$.

Characterisation of manufacturing ZnO nanoparticle

Manufacturing compounds were analysed using X-ray diffraction to identify the structure and purity of ZnO nanoparticles (Shimadzu, Japan) using the spectral range of 25-50 2θ . Detection of light scattering from matter is a beneficial method with applications in several clinical disciplines, relying on the light supply and detector. 1 mL distilled water turned into the cell, after which 50 μL from stock dispersions was added. Length distributions of the nanoparticles were

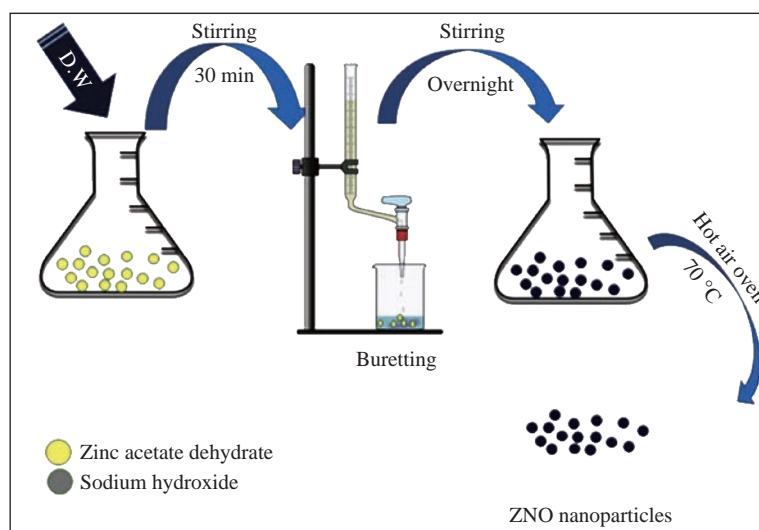


Fig. 1 Chemical steps of ZnO nanoparticles synthesis.

identified through the dynamic light scattering (DLS) method. Finally, scanning electron microscopy SEM (GENEX, USA) and transmission electron microscopy TEM (Philips EM) analyses were conducted to determine the particle size and morphology.

Anticancer activity

Cytotoxicity determination using MTT assay

To determine the cell killing effect of nano ZnO, MTT assay was used according to Suliaman, et al. [12]. Human breast cancer cell lines (MCF-7) were seeded at 7000-10000 cells/well after 24 h or confluent monolayer was achieved. Cells were treated with nano ZnO at fold dilutions from 100-6.25 $\mu\text{g/mL}$ in culture media. Cell viability was measured at 72 h of exposure by removing the medium, adding 50 μL of MTT stain and incubating for 2 h at 37 °C. After removing the stain, it was washed with phosphate-buffered saline (PBS). The absorbency was determined on a microplate reader at 492. The assay was performed in triplicate.

Clonogenicity

The cells line were plated in 12 well plates at the density of 1000 cells/mL. After 24 h, the cells were treated with zinc oxide nanoparticles with IC_{50} concentration. After that, the medium was removed and the cell rinsed using PBS solution. The colonies were fixed and stained using crystal violet, then washed to remove excessive dye using distal water and then photographed [13].

Nuclear Morphology change detection using DAPI stain

DAPI assay was done to visualize the nuclear morphological change of ovarian cells using 365-nm filter of fluorescent microscopy. The cells were treated with zinc oxide nanoparticles with IC_{50} concentration and followed with incubation for 48 h. The wells were rinsed with filtered PBS, then, the cells fixed with absolute ethanol for 0.5 h. After that, washing required with distilled water. The cells were stained using DAPI stain solution for 30 min, the rinsed required to remove the excess stain using distilled water [14]. The nuclear changes visualized using 40 \times power of a fluorescence microscope.

Acridine orange/ethidium bromide (AO/EB) dual staining

AO/EB double staining assay was used to identify the cellular death. Acridine orange was taken up via

viable cells and emitted green fluorescence. Ethidium bromide was taken up only via nonviable cells and emitted red fluorescence through intercalation with harm DNA [15]. Cells line was seeded with density (1×10^4) on the cover slide that was located at the 12-well plate with ZnO nanoparticles. After 48 h of incubation, the medium was removed and aliquot of 20 μL from dye mixture was combined with 100 μL cell suspension in a well plate. After the incubation period for 15-30 min, the cover slides were taken for observation under fluorescent microscope 100 \times magnification.

Gene alteration detection using real-time (RT) quantitative polymerase chain reaction (PCR)

Gene alteration of cell line was investigated using real-time quantitative PCR. In this experiment, three main types of gene were measured to identify the pathway of apoptosis and the mechanism action. These genes included p53, caspase-9 and caspase-8. RT-PCR was accomplished to investigate the modifications in hippocampal expression genes. The primer sets were designed based totally on the sequences from the NCBI database. The sequences of primers used within the quantitative RT-PCR assay included:

- (1) P53 (forward: 5'-CCGTCCCAAGCAATGGATG-3') (reverse: 5'-GAAGATGACAGGGGCCAGGAG-3');
- (2) Caspase-8 (forward: 5'-GACCACGACCTTTGAAGAGCTTC-3') (reverse: 5'-CAGCCTCATCCGGGATATATC-3') ; and (3) Caspase-9 (forward: 5'-CTCTTGAGCAGTGGCTGGTC-3') (reverse: 5'-GCTGATCTATGAGCGATACT-3').

Each RT-PCR reaction combination contained 1 μL cDNA, 7.5 μL SYBR green, 0.3 μL ROX, and 0.3 μL related primers; the final quantity was topped up to 15 μL via adding 5.6 μL of distilled water. The assay was performed with SYBR Premix Ex. TaqTM kit. The real-time detection of emission intensity of SYBR green reacted to double-stranded DNAs and was performed via the implemented Biosystems ABI PRISM Sequence Detection System. GAPDH mRNA was used as an inner control to identify the relative expression amount of genes.

Immunofluorescence microscopy

MCF-7 cells were stimulated as indicated. The cells were with 1 \times PBS, then fixed with 4% paraformaldehyde (PFA) for 30 min at room temperature, and then permeabilized in 0.5% Triton-X for 30 min at room temperature. The permeabilized

cells were blocked with 10% normal goat serum for 30 min. The primary antibody was added to cells for 24 h at 4 °C. The antibodies were 1 mg/mL anti-p53 and 1 mg/mL anti-caspase-8. After washing three times with $1 \times$ PBS, the secondary antibodies were added for 120 min at room temperature. The antibodies were 1 mg/mL Alexa Fluor 488-conjugated goat anti-rabbit IgG or 1 mg/mL Alexa Fluor 568-conjugated goat anti-mouse IgG. The cells were washed three times with PBS, and viewed using a fluorescent microscope.

Statistical analysis

The study data were presented as means \pm standard error of the mean. The statistical analyses were performed using the GraphPad Prism 5 software package (GraphPad Software, Inc. San Diego, California).

Results and Discussion

Characterization of manufactured ZnO nanoparticles

X-ray powder diffraction (XRD) analysis of ZnO film samples was accomplished with variety 25-500 using $\text{Cu}\alpha$ radiation. Fig. 2 visualized an XRD of ZnO film samples having numerous peaks of ZnO nanoparticle, indicating random orientation for the polycrystalline nature and measured inter planer distances. The higher peak intensities of an XRD were because of the higher crystallinity, and the larger grain length might be attributed to the agglomeration of particles [16]. The pointy diffraction sample suggested that the sample revealed hexagonal ZnO crystalline shape with lattice consistent of $a = 3.256$ Å and $c = 5.31$ Å, which was stated in JCPDS (36-1451) for bulk ZnO. DLS technique was used to determine Brownian motion of spherical dispersed particles and to narrate this to the hydrodynamic

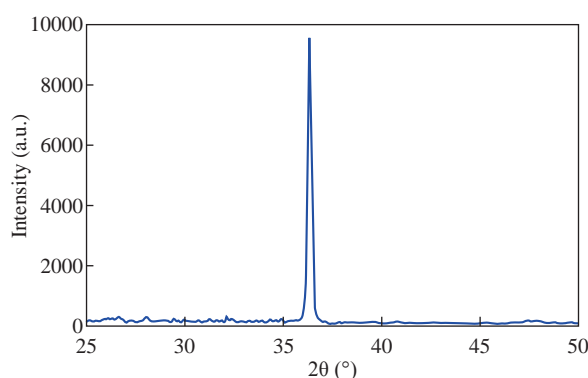


Fig. 2 X-ray diffraction analysis of ZnO nanoparticles.

length of the particles within the dispersed solution via dynamic fluctuations of scattered light intensity. This scattered light intensity was similarly mathematically manipulated to relate the hydrodynamic length of the debris. A vital characteristic of Brownian motion measured with the aid of DLS was that small debris circulated quicker in assessment to large debris, and the relationship between the dimensions of a particle and its velocity due to Brownian motion was defined within the Stokes-Einstein equation. As visualized in Fig. 3, ZnO NPs diameter was within the range of 4-10 nm. The morphology and the scale of the manufactured zinc oxide nanoparticles were detected via SEM and TEM. As visualized in Fig. 4(a) and (b), the morphology of the zinc oxide nanoparticles under identical magnifications, the images show that the ZnO nanoparticles were round in shape and the average diameter ranged from 10-15 nm.

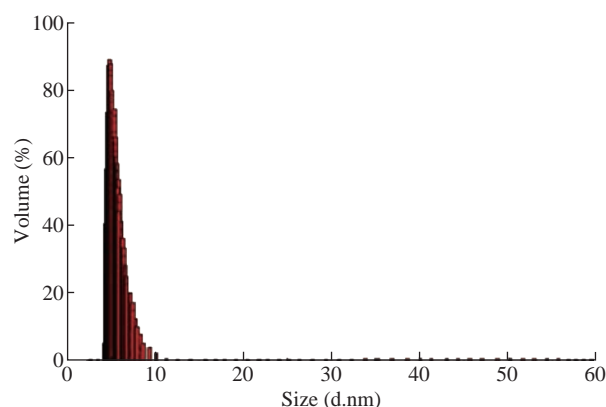


Fig. 3 DLS histogram image of ZnO nanoparticles.

Cytotoxicity determination using MTT assay

Fig. 5 shows the viability results examined by MTT colorimetric assay with human breast cancer cell MCF-7 after 72 h of exposure with different concentrations of ZnO nanoparticles at concentrations from 100 to 6.25 $\mu\text{g}/\text{mL}$, and the cytotoxicity was then determined using MTT assay. For human breast cancer cell line (MCF-7), the results illustrated that treatment with ZnO nanoparticles inhibited the growth of cells significantly ($P \leq 0.05$) and the reduction was concentration-dependent. The inhibitory concentration value (IC_{50}) of ZnO nanoparticles was 15.88 $\mu\text{g}/\text{mL}$ as visualized in Fig. 4-8. ZnO nanoparticles, with their specific properties which include biocompatibility, excessive selectivity, greater cytotoxicity and smooth synthesis, can be a promising anticancer agent [17].

ZnO nanoparticles have the specific capability to

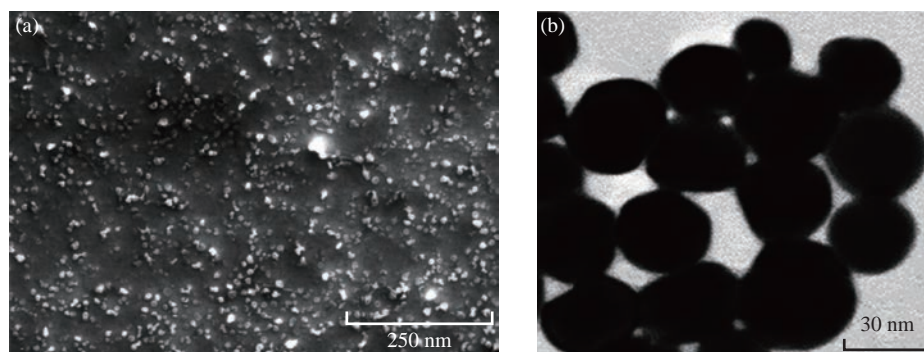


Fig. 4 (a) SEM and (b) TEM image of ZnO nanoparticles showing uniformly distributed nanoparticles with spherical shape.

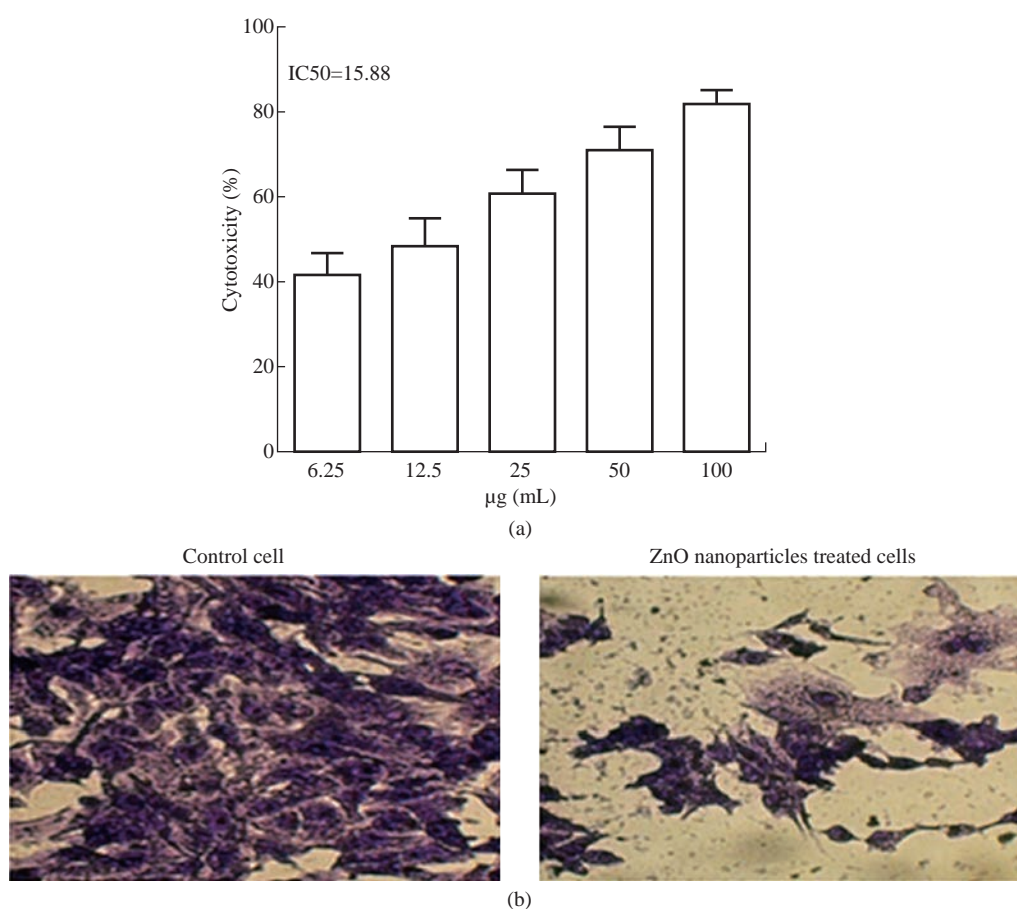


Fig. 5 Cytotoxicity and antiproliferative activity of ZnO nanoparticles in MCF-7 cells. (a) MTT assay, the values represent mean \pm S.E.; (b) Treated cell for 24 h, then stained with crystalviolet imaged by inverted phase contrast microscope.

evoke oxidative stress in most cancers cells, which has been observed to be one of the mechanisms of cytotoxicity of ZnO nanoparticles closer to cancer cells. This property is due to the semiconductor nature of ZnO; conduction of electricity power takes vicinity via the motion of unfastened electrons inside the valence band [18].

Clonogenicity assay

As visualized in Fig. 6, the anti-proliferative efficiency on human breast cancer cell MCF-7

through the use of clonogenic assay was determined to similarly verify the inhibition activity to tumor cells. Colony formation assay is an in-vitro cell survival assay based totally on the capacity of a single cell to develop right into a colony [19]. It may be used to identify the effectiveness of different cytotoxic agents. ZnO nanoparticles exhibited principal performance at the colony formation cell line at IC_{50} concentration. The discount of colony formation may also lead to that the cancer cells within the continuous remedy were killed in the first 48 h of treatment, suggesting that

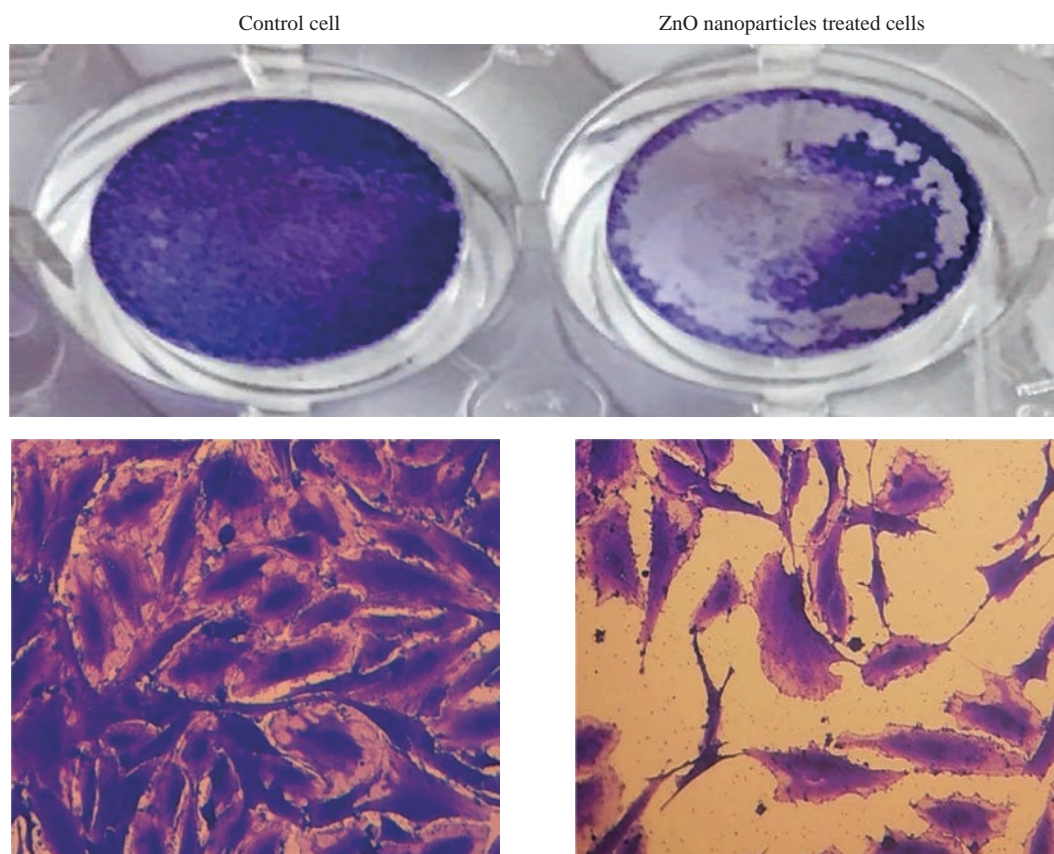


Fig. 6 Effects of ZnO nanoparticles in clonogenicity of MCF-7 cell line.

ZnO nanoparticles have been taken up by way of cells and evoke the death mechanism. Consequently, the result may also display that the synthesis compound ought to set off cell death. However, the mechanism of cell dying is not genuinely understood and requires extra analysis to research the mechanism.

Nuclear morphology change detection using DAPI stain

To evaluate the cytotoxicity effects of the manufactured compounds effect at nuclear of the cell line, the changes inside the nuclear

morphology were tested after exposing with IC_{50} of ZnO nanoparticles as illustrated in Fig. 7. In assessment, apoptosis was characterized by using cell shrinkage, preservation of plasma membrane integrity, chromatin condensation, and nuclear fragmentation. Generally, the results suggested that ZnO nanoparticles could induce apoptosis in breast cell line. The discount of cell line growth frequently included amendment of various key signaling pathways, which ended up because of disturbance in apoptotic process or cell cycle and resulted in impact on the mRNA gene expression [20].

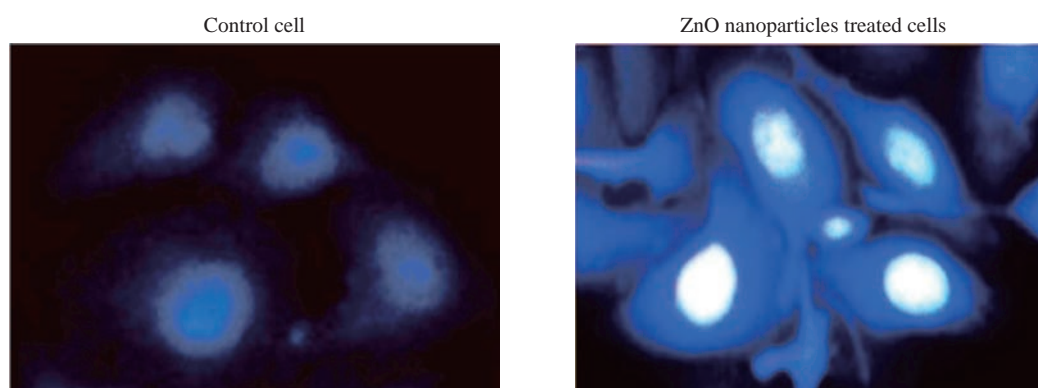


Fig. 7 Fluorescence microscopy images of MCF-7 cell line using DAPI stain showing apoptosis.

Acridine orange/ethidium bromide (AO/EB) dual staining

AO/EB analysis was employed to examine the changes in nuclear morphology of human breast cancer cell MCF-7 treated cells. The apoptotic cells were indicated based on DNA damage. AO/EB dual staining was used to determine distinct apoptotic signs characteristics of nucleate alternations. Viable and non-apoptotic cells appeared green, while apoptotic cells appeared orange or red. As shown in Fig. 8, exposing cells to ZnO nanoparticles caused an increase in membrane disruption and formation of lysosomes vacuoles compared to untreated control cells. The excessive capacity to cause dying to the cell is associated with the capability of nanoparticle to penetrate via the cellular membrane and impact at the mRNA expression of suppression gene that cause increase in the production level of reactive oxygen species (ROS) within the cell [21]. With expanded levels of ROS and oxidative stress, ZnO NPs display a deleterious impact at the lipid, protein and nucleic acid of the cell [22]. Increased ROS can cause membrane

damage via lipid peroxidation and protein denaturation, ensuing in cell dying via necrosis and DNA Strand damage, resulting in cellular dying via process called apoptosis [23].

Zinc oxide nanoparticles upregulates caspase-8 and p53

In this study, quantitative real-time PCR was used to identify the change in the expression of the mRNA of apoptotic genes (p53, caspase-8 and caspase-9) in cells that were exposed to ZnO nanoparticles for 24 h with concentrations of 6.25, 12.5 and 25 $\mu\text{g/mL}$. The PCR results revealed that apoptotic markers at the mRNA level were altered and dealt with cell lines due to ZnO nanoparticles remedy. The mRNA level of tumor suppression gene p53 showed an increase as visualized in Fig. 9(a) in treated cells; the level of p53 increased dependently on the concentration. Moreover, the performance of ZnO nanoparticles at the mRNA expression of caspase-8 and caspase-9 was observed. The expression of caspase-9 was downregulated at 24 h as shown in Fig. 9(c), while caspase-8 was upregulated in treated cells in comparison

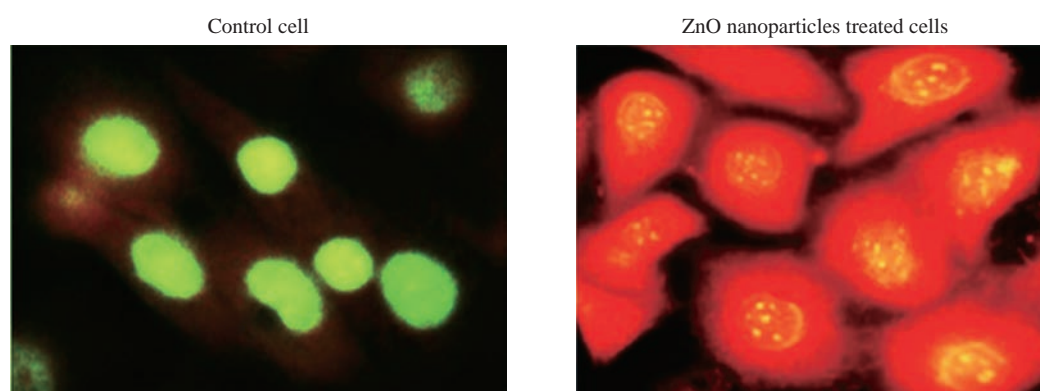


Fig. 8 Fluorescence microscopy images of MCF-7 cell lines stained with AO and EB in the presence and absence of Zinc oxide nanoparticles.

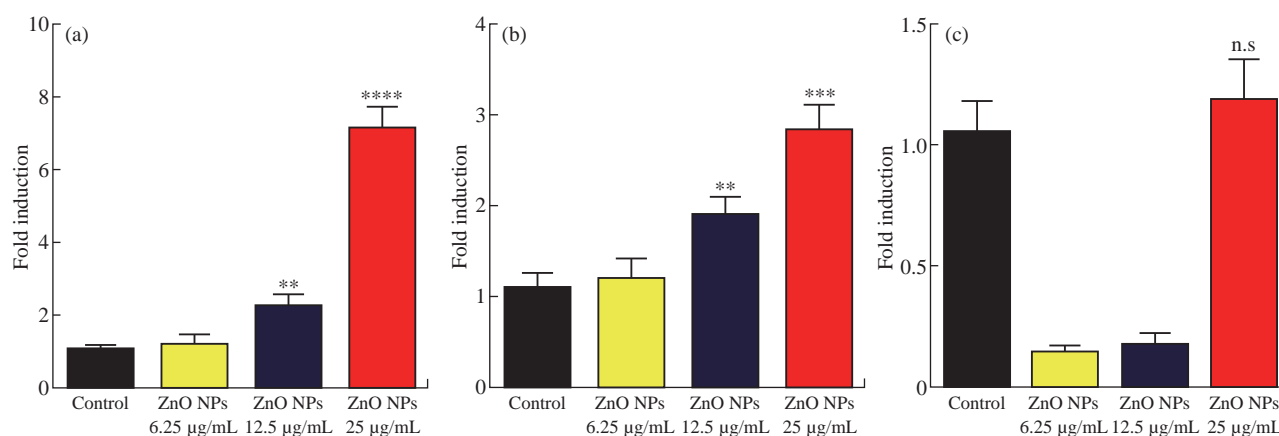


Fig. 9 Zinc oxide nanoparticles and their role in the apoptotic genes expression : (a) p53; (b) caspase-8 ; and (c) caspase-9. The values represent mean \pm S.E. **P < 0.01, ***P < 0.001.

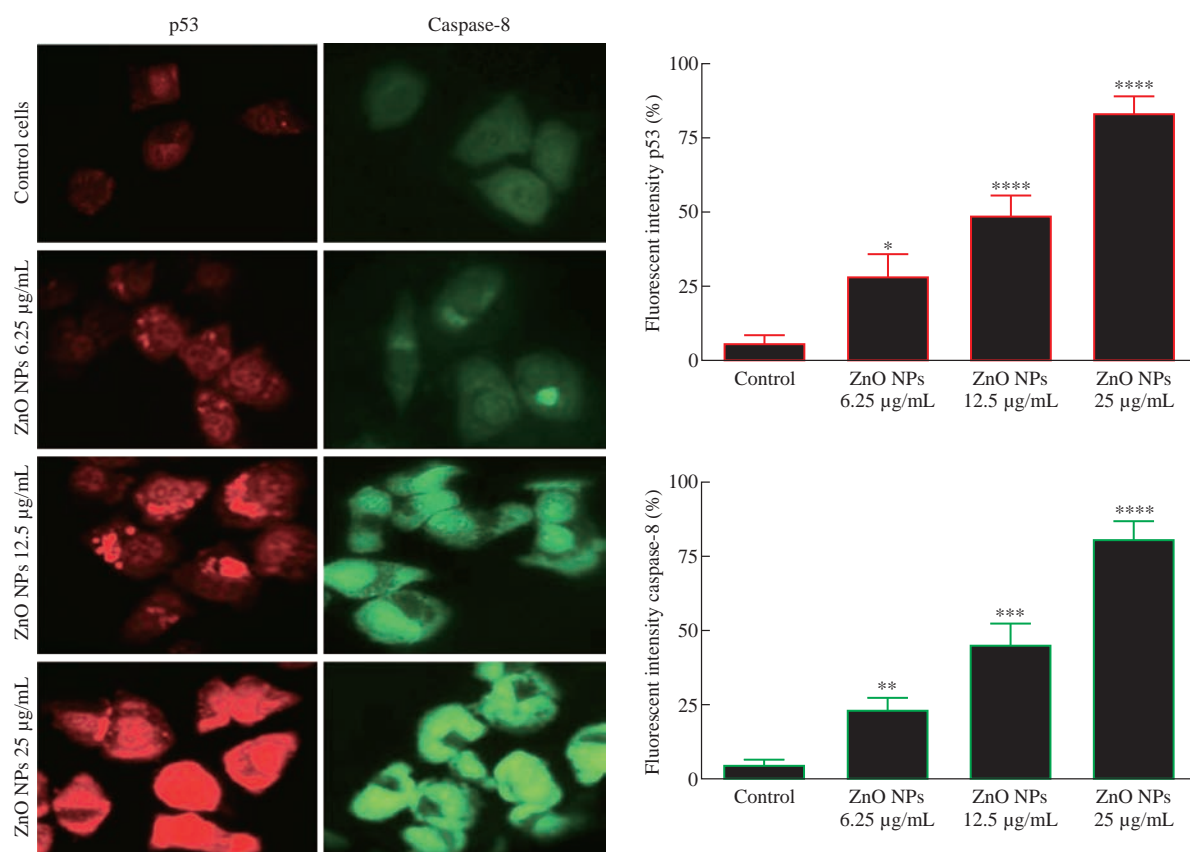


Fig. 10 Immunofluorescence result of p53 and caspase-8 in MCF-7 cells. Cells were left untreated as a control, or treated with ZnO NPs as indicated. Cells were fixed, permeabilized, and then stained with primary and secondary antibodies. (Scale bar = 10 µm. Graphs represent percentage of fluorescent intensity using Image J software. Asterisks indicate statistical difference from control cells. Columns are mean of three independent experiments. Error bars are $M \pm SE$. * $p < 0.05$; ** $p < 0.01$; *** $p < 0.001$.)

with untreated control cells at 24 h of treatment as visualized in Fig. 9(b). The tumor suppressor p53 gene and caspase enzyme assist to investigate cells frequently and save them from becoming cancerous [24]. If a cell indicates any form of malignancy, a DNA repair mechanism is activated to restore the altered DNA [25]. Zinc is one of the co-factors of those enzymes and performs a vital function in host defense in opposition to the initiation and development of cancer [26]. The particular DNA-binding domain of p53 consists of a complicated tertiary structure that is stabilized via zinc [27]. Consequently, zinc performs a main function in maintaining the interest of tumor suppressor gene p53 and performs a vital role within the activation of the caspase-8 enzyme, a main enzyme accountable for apoptosis [28]. Caspase-9 is the touchy apoptosis-associated molecular target of zinc [29]; it is responsible for the activation of caspase-3 and different enzymes which are liable for nuclear membrane dissolution leading to cellular dying. Zinc performs a crucial role in response to oxidative stress, DNA replication, DNA harm repair, cell cycle development and apoptosis; as a result a deficiency of

zinc ends in disruption of important homeostasis in cells [30, 31]. To confirm that ZnO NPs' up-regulated induction of p53 and caspase-8 and that the phenomena is concentration manner, immunofluorescent assay was conducted according to manufacturer's protocol. Fig. 10 represents a p53 and caspase-8 induction in MCF-7 cells after treated with ZnO NPs at different concentrations as indicated. The fluorescence of p53 and caspase-8 was very low in control cells, while it was very clear in p53 and caspase-8 treated MCF-7 cells, which suggested that ZnO NPs were able to induce apoptosis.

Conclusions

Nanoparticles including ZnO have been examined and developed for cancer therapy. Lately, numerous research corporations have suggested the usage of ZnO nanoparticles as anti-cancer therapeutic drug. In this study, cytotoxicity of ZnO nanoparticles to human breast cancer cells was investigated. The results confirmed that exposure of ZnO nanoparticles to cancer cells led to causing considerable cytotoxicity.

The findings proposed that ZnO nanoparticles had high activity within the induction of genes expression. Consequently, ZnO nanoparticles chemoprevention may be efficacious for the prevention and remedy of numerous cancers.

Conflict of Interests

The authors declare that no competing interest exists.

References

- [1] N.G. Zaorsky, T. Churilla, B. Egleston, et al., Causes of death among cancer patients. *Annals of Oncology*, 2016, 28(2): 400-407.
- [2] A. Adjiri, Identifying and targeting the cause of cancer is needed to cure cancer. *Oncology and Therapy*, 2016, 4(1): 17-33.
- [3] A.K. Thomson, J.S. Heyworth, J. Girschik, et al., Beliefs and perceptions about the causes of breast cancer: a case-control study. *BMC Research Notes*, 2014, 7(1): 558.
- [4] A.K. Biswas, M.R. Islam, Z.S. Choudhury, et al., Nanotechnology based approaches in cancer therapeutics. *Advances in Natural Sciences: Nanoscience and Nanotechnology*, 2014, 5(4): 043001.
- [5] B.V. Bonifácio, P.B. da Silva, M.A. dos Santos Ramos, et al., Nanotechnology-based drug delivery systems and herbal medicines: A review. *International Journal of Nanomedicine*, 2014, 9: 1.
- [6] I. Khan, K. Saeed, Nanoparticles: Properties, applications and toxicities. *Arabian Journal of Chemistry*, 2017.
- [7] T.G. Smijs, S. Pavel, Titanium dioxide and zinc oxide nanoparticles in sunscreens: focus on their safety and effectiveness. *Nanotechnology, Science and Applications*, 2011, 4: 95.
- [8] S. Chaudhary, A. Umar, K. Bhasin, et al., Chemical sensing applications of ZnO nanomaterials. *Materials*, 2018, 11(2): 287.
- [9] A. Kołodziejczak-Radzimska, T. Jesionowski, Zinc oxide - From synthesis to application: A review. *Materials*, 2014, 7(4): 2833-2881.
- [10] J. Qi, H. Zhang, S. Lu, et al., High performance indium-doped ZnO gas sensor. *Journal of Nanomaterials*, 2015, 16(1): 74.
- [11] M.F. Khan, A.H. Ansari, M. Hameedullah, et al., Sol-gel synthesis of thorn-like ZnO nanoparticles endorsing mechanical stirring effect and their antimicrobial activities: Potential role as nano-antibiotics. *Scientific Reports*, 2016, 6: 27689.
- [12] G.M. Sulaiman, M.S. Jabir, and A.H. Hameed, Nanoscale modification of chrysin for improved of therapeutic efficiency and cytotoxicity. *Artificial Cells, Nanomedicine, and Biotechnology*, 2018: 1-13.
- [13] S. Elangovan, T.C. Hsieh, and J.M. Wu, Growth inhibition of human Mda-Mb-231 breast cancer cells by Δ -tocotrienol is associated with loss of cyclin D1/Cdk4 expression and accompanying changes in the state of phosphorylation of the retinoblastoma tumor suppressor gene product. *Journal of Anticancer Research*, 2008, 28(5A): 2641-2647.
- [14] M.S. Jabir, G.M. Suliman, Z.J. Taqi, et al., Iraqi propolis increases degradation of IL-1b and NLR4 by autophagy following *Pseudomonas aeruginosa* infection. *Microbes and Infection*, 2018, 18: 89-100.
- [15] M.S. Jabir, A.A. Taha, and U.I. Sahib, Linalool loaded on glutathione-modified gold nanoparticles: a drug delivery system for a successful antimicrobial therapy. *Artificial Cells, Nanomedicine, and Biotechnology*, 2018: 1-11.
- [16] J. Hasnidawani, H. Azlina, H. Norita, et al., Synthesis of ZnO nanostructures using sol-gel method. *Procedia Chemistry*, 2016, 19: 211-216.
- [17] G. Bisht, S. Rayamajhi, ZnO nanoparticles: A promising anticancer agent. *Nanobiomedicine*, 2016, 3: 9.
- [18] P. Rodnyi, I. Khodyuk, Optical and luminescence properties of zinc oxide. *Optics and Spectroscopy*, 2011, 111(5): 776-785.
- [19] T. Miyashita, Y. Higuchi, M. Kojima, et al., Single cell time-lapse analysis reveals that podoplanin enhances cell survival and colony formation capacity of squamous cell carcinoma cells. *Scientific Reports*, 2017, 7: 39971.
- [20] R. Sever, J.S. Brugge, Signal transduction in cancer. *Cold Spring Harbor Perspectives in Medicine*, 2015, 5(4): a006098.
- [21] D.D. Ma, W.X. Yang, Engineered nanoparticles induce cell apoptosis: Potential for cancer therapy. *Oncotarget*, 2016, 7(26): 40882.
- [22] S. Vidovic, J. Elder, P. Medihala, et al., ZnO nanoparticles impose a panmetabolic toxic effect along with strong necrosis, inducing activation of the envelope stress response in *Salmonella enterica* serovar enteritidis. *Antimicrobial Agents and Chemotherapy*, 2015, 59(6): 3317-3328.
- [23] M. Nita, A. Grzybowski, The role of the reactive oxygen species and oxidative stress in the pathomechanism of the age-related ocular diseases and other pathologies of the anterior and posterior eye segments in adults. *Oxidative Medicine and Cellular Longevity*, 2016, 2016.
- [24] M. Olsson, B. Zhivotovsky, Caspases and cancer. *Cell Death and Differentiation*, 2011, 18(9): 1441.
- [25] H. Erasmus, M. Gobin, S. Niclou, et al., DNA repair mechanisms and their clinical impact in glioblastoma. *Mutation Research/Reviews in Mutation Research*, 2016, 769: 19-35.
- [26] D. Dhawan, V.D. Chadha, Zinc: A promising agent in dietary chemoprevention of cancer. *The Indian Journal of Medical Research*, 2010, 132(6): 676.
- [27] O. Laptenko, I. Shiff, W. Freed-Pastor, et al., The p53 C terminus controls site-specific DNA binding and promotes structural changes within the central DNA binding domain. *Molecular Cell*, 2015, 57(6): 1034-1046.
- [28] K.W. Ng, S.P. Khoo, B.C. Heng, et al., The role of the tumor suppressor p53 pathway in the cellular DNA damage response to zinc oxide nanoparticles. *Biomaterials*, 2011, 32(32): 8218-8225.
- [29] K.L. Huber, J.A. Hardy, Mechanism of zinc - mediated inhibition of caspase9. *Protein Science*, 2012, 21(7): 1056-1065.
- [30] S. Alam, S.L. Kelleher, Cellular mechanisms of zinc dysregulation: a perspective on zinc homeostasis as an etiological factor in the development and progression of breast cancer. *Nutrients*, 2012, 4(8): 875-903.
- [31] R. Madabhushi, L. Pan, and L.H. Tsai, DNA damage and its links to neurodegeneration. *Neuron*, 2014, 83(2): 266-282.

Copyright© Haitham Ali Kadhem, Sumayah Abdhussien Ibraheem, Majid Sakhi Jabir, Afraa Ali Kadhim, Zainab Jihad Taqi, and Mihailescu Dan Florin. This is an open-access article distributed under the terms of the Creative Commons Attribution License, which permits unrestricted use, distribution, and reproduction in any medium, provided the original author and source are credited.